Using large-scale NO_2 data from citizen science for air quality compliance and policy support

*De Craemer Sam[1,2], Vercauteren Jordy[3], Fierens Frans[4], Wouter Lefebvre[2], Meysman J.R. Filip[1,5,]**

[1] Department of Biology, University of Antwerp, Universiteitsplein 1, B-2610 Wilrijk, Belgium

[2] VITO, Boeretang 200, 2400 Mol, Belgium

[3] Vlaamse Milieumaatschappij, Kronenburgstraat 45, 2000 Antwerpen, Belgium

[4] Belgian Interregional Environment Agency, Gaucheretstraat 92-94, 1030 Brussels, Belgium

[5] Department of Biotechnology, Delft University of Technology, Van der Maasweg 9, 2629 HZ Delft, The Netherlands

* Corresponding author: filip.meysman@uantwerpen.be

Abstract: 173 words, Main text : 5115 words, Figures & tables: 1500. Total: 6788

Key words

Air quality, citizen science, nitrogen dioxide, passive sampler, policy support

Abstract

Citizen science projects that monitor air quality have recently drastically expanded in scale. Projects involving thousands of citizens generate spatially dense datasets using low-cost passive samplers for nitrogen dioxide (NO_2), which complement data from the sparse reference network operated by environmental agencies. However, there is a critical bottleneck in using these citizen-derived datasets for air quality policy. The monitoring effort typically lasts only a few weeks, while long-term air quality guidelines are based on annual averaged concentrations that are not affected by seasonal fluctuations in air quality. Here, we describe a statistical model approach to reliably transform passive sampler NO_2 data from multi-week averages to annual averaged values. The predictive model is trained with data from reference stations that are limited in number but provide full temporal coverage, and is subsequently applied to the one-off dataset recorded by the spatially extensive network of passive samplers. We verify the assumptions underlying the model procedure, and demonstrate that model uncertainty complies with the EU quality objectives for air quality monitoring. Our approach allows a considerable cost-optimization of passive sampler campaigns and removes a critical bottleneck for citizen-derived data to be used for compliance checking and air quality policy use.

1. Introduction

Air quality remains an important environmental problem, as 92% of the global population lives in areas where pollutant levels exceed health-based standards for ambient air quality **(1)**. To support air quality policies, environmental protection agencies (EPAs) have developed systematic monitoring programs, which involve a network of reference stations that provide a continuous data stream for a wide array of air pollutants **(2).** However, the construction and maintenance of these

reference stations is resource intensive, and hence EPA networks only include a limited number of stations **(3)**. Especially in urban environments, traffic-related air pollution like NO_2 can vary over small distances **(4–6)**, and so data from a single monitoring station can only be considered representative of a small surrounding area **(7–9)**. To obtain a more detailed insight into the small-scale variation of air quality, complementary methods are needed that enable the low-cost collection of datasets with high spatial resolution. Such spatially dense datasets are critical for the validation and improvement of air quality models that are used for policy guidance, while they also allow to investigate the spatial representativeness of the reference stations included in official monitoring networks **(10,11).**

Passive NO_2 samplers enable the collection of spatially distributed data in cost-efficient manner **(12)**, while retaining sufficient data quality **(13,14)**, and have been used in local networks of 50-100 samplers by governmental agencies and researchers to measure NO_2 levels complementary to reference stations (e.g. **15–17**). Very recently, the scale at which these NO_2 passive samplers are used has greatly expanded, through citizen science projects involving up to 20.0000 participants, which monitor the air quality outside their house **(18–20)**. However, the policy use of these citizen science data is currently strongly hampered by the particular way these citizen science projects are conducted. Citizen-based passive sampler campaigns are typically executed only once, and the monitoring period is relatively short (e.g. 1-4 weeks for NO_2 in an urban context) to avoid that passive samplers become saturated **(21)**. Consequently, citizen-derived datasets typically produce NO_2 concentrations averaged over multiple weeks. In contrast, compliance checking for NO_2 with guideline values of the World Health Organisation (WHO) or legal limit values requires averaging periods of 1 hour or 1 year **(22,23)**. Additionally, annual averaged NO_2 values also require a regularly distributed measurement effort throughout the year **(23)**. Data collected within citizen

science projects do not meet these criteria, and so, these data cannot be directly implemented for compliance checking.

Here, we describe an extrapolation method to reliably obtain annual averages from time-limited NO_2 passive sampler measurements. Our model approach builds upon previous observations that spatial patterns of NO_2 remain remarkably stable in time across urban regions **(6,16,17,24–26)**. Different extrapolation models are tested, and the uncertainty associated with each model approach is quantified. Additionally, the effect of the sampling period on the model uncertainty is evaluated, allowing insight in the optimal experimental design of sampler campaigns. We evaluate our results with respect to EU standards for air quality monitoring.

2. Methods

2.1. Rationale of the model approach

We consider a certain geographical domain (e.g. city or region) over which air quality is monitored by a network of reference monitoring stations (N_R sites), complemented with an additional dense network of passive samplers (N_S sites) – Fig. 1 shows a real world example. The reference network is sparse ($N_R << N_S$), but provides continuous NO_2 data at high temporal resolution, which allows to extract both monthly averages (X_i^R for i=1.. N_R) and annual averages (Y_i^R for i=1.. N_R). The passive sampler network has a high spatial resolution, but only provides averaged data for over a restricted period of multiple weeks (X_j^S for j=1.. N_S). The objective is to construct a predictive model based on the reference data (X_i^R and Y_i^R) and apply this model to the passive sampler locations, thus predicting Y_j^S from X_j^S (Fig. 1c). The predictive model is hence trained with data from reference stations that are limited in number but provide full temporal coverage, and is subsequently applied to the large, one-off dataset from the passive samplers.

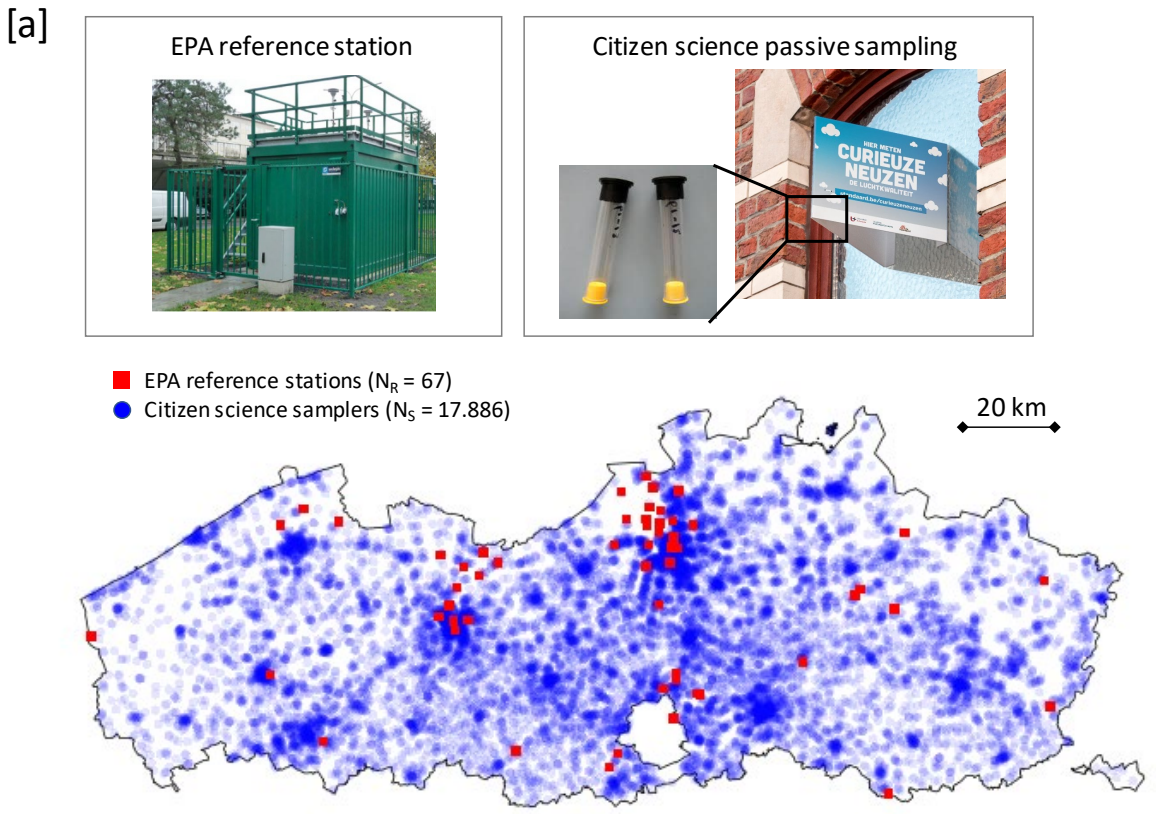
[a]
EPA reference station
Citizen science passive sampling
CURIEUZE NEUZEN
EPA reference stations (N_R = 67)
Citizen science samplers (N_S = 17.886)
20 km
[b]
NO_2 (30 min average)
S1
S2
S3
S4
S5
rural
urban
value at present
value at next time step
NO_2 (4 week average)
S1
S2
S3
S4
S5
rural
urban
[c]
Model-based extrapolation procedure
EPA hourly reference data
INPUT
Citizen science sampler data
averaging
4 week average X_i^R
statistical model
yearly average Y_i^R
4 week average X_j^S
apply model
yearly average Y_j^S
OUTPUT
Extensive spatial dataset of yearly averaged NO_2

88

89 **Figure 1.** [a] Map showing the N_R = 67 reference stations (red squares) operated by the Flanders
90 Environment Agency (Vlaamse Milieumaatschappij, VMM) in the monitoring network across the
91 region of Flanders (Belgium). The map also shows locations at which 4-weekly averaged NO_2 data
92 were collected in the citizen science project CurieuzeNeuzen via passive samplers (N_S = 17.886
93 data locations - blue dots). [b] Schematic illustration of the difference in spatial correlation
94 between both short-term (30 min averaged) and long-term (4 week averaged) NO_2 variations. A
95 fictitious monitoring network consists of 5 stations (S1 to S5) with different NO_2 levels typifying
96 spatial variability. Short-term fluctuations show little correlation between stations, while long-term
97 fluctuations show large correlation. [c] Model-based extrapolation procedure to calculate annual
98 averaged sampler data from multi-week averaged sampler data.

99 The central premise of our model approach is illustrated in Fig. 1b. The NO_2 concentration at a
100 given site within a monitoring network will be determined by the interplay of production (e.g.
101 traffic emissions), transport (e.g. upwind supply and dispersal) and removal (e.g. washout with
102 precipitation or photochemical oxidation). The relative strength of these processes will differ
103 between sites, thus giving rise to spatial variability (i.e. differences in NO_2 concentrations between
104 stations S1 to S5). Additionally, the NO_2 concentration at a given site will show both short-term
105 and long-term variations, and the key assumption underlying our model approach is that these two
106 types of variations will have different drivers. Short-term variations (minutes to days) can be
107 driven by site-specific changes in local emissions (e.g. a temporary traffic jam) or meteorological
108 conditions (e.g. a local rain shower). As a result, short-term NO_2 variations will tend to show little
109 correlation between sites (Fig. 1b). In contrast, longer-term variations (weeks to years) are mostly
110 driven by changes in weather (e.g. seasonal variation in atmospheric boundary layer) or economic
111 activity (e.g. summer holidays). If these impacts of meteorology and economy are similar across

112 the spatial domain examined, then long-term NO_2 variations will be correlated between sites (Fig.
113 1b). Consequently, when averaged over a sufficiently long period, the site-specific short-time
114 variations will be filtered out, and what remains are long-term effects that commonly influence all
115 stations. Therefore, one expects the long-term averaged NO_2 levels to move up and down in a
116 synchronous way at different locations, thus preserving the spatial pattern (Fig. 1b lower panel).
117 Moreover, if a period of a few weeks is sufficient to filter away short-term effects, one also
118 expects a predictable model relation between multi-week-averaged and annual averaged NO_2
119 concentrations that is similar across the whole monitoring domain (due to temporal stability of
120 inter-site variations). If this hypothesis holds, we can use following multi-step model approach to
121 map multi-week sampler data onto annual averages (Fig. 1c):

122 1. Collect multi-week-averaged NO_2 for the many (N_S) stations in the passive sampler
123 network, thus providing the raw sampler dataset ($X_j^{S,raw}$). Ensure that a subset of the
124 passive samplers is co-located at a limited number (N_R) of reference stations.
125 2. Determine the time-averaged NO_2 value for the limited number (N_R) of reference stations
126 over the same time period as the passive sampler campaign (X_i^R data).
127 3. Calibration model. Develop a statistical regression between the X_i^R reference data and
128 the raw multi-week NO_2 data of the co-located passive samplers.
129 4. Apply the calibration model to all N_S raw sampler data to obtain the calibrated sampler
130 dataset X_j^S.
131 5. Determine the time-averaged annual NO_2 value for the reference stations over the year
132 that contains the passive sampler campaign (Y_i^R data)
133 6. Extrapolation model. Develop a statistical regression between the independent variable
134 X_i^R and the outcome variable Y_i^R for the N_R reference stations

7. Apply this extrapolation model to the N_S sampler stations to obtain the annual averaged estimate Y_j^S from the calibrated multi-week-averaged X_j^S data for each station in the passive sampler network.

The proposed model approach hence includes both a calibration step and extrapolation step. The need for calibration has already been extensively documented in previous studies (see reviewed in **21**). While passive samplers are generally precise, they often show a systematic bias when compared to reference data. Calibration based on co-location at reference stations is hence an essential step in the quality assurance procedure of passive sampler data (**21**), and thus must also be implemented within citizen science projects using passive samplers **(18,19)**. In this study, we focus on the extrapolation step, which is the novel part of the proposed model approach.

2.2. Datasets

We tested the extrapolation model step with two datasets for which both multi-week as well annual averaged NO_2 data were available (thus enabling model cross-validation, as further discussed below). The first dataset includes hourly-averaged NO_2 concentrations (measured by chemiluminescence) from the 67 reference stations that make up the regular monitoring network within the region of Flanders (Belgium) (Fig. 1a). This so-called "monitor dataset" spans a period of 8 consecutive years from 1 January 2011 to 31 December 2018. We used this dataset to verify whether NO_2 concentrations at different locations in a geographical area show similar long-term temporal trends.

The second dataset includes NO_2 concentrations that were obtained via Palmes diffusion tubes **(12)** over consecutive 2-week sampling periods. Passive samplers were co-located at a subset of 24 stations within the reference monitoring network of Flanders. In order to reduce sampler bias,

158 NO_2 concentrations from passive samplers were calibrated by orthogonal regression against the
159 data from the reference stations at which they were co-located **(21)**. This so-called "sampler
160 dataset" spans a period of 1 year and consists of 26 consecutive measurement periods of two
161 weeks, lasting from 28 December 2017 until 26 December 2018. NO_2 sampler data are reported
162 as the mean of 2-4 replicates at each station and time point. Due to analytical problems, data from
163 periods 4 and 5 (8 February to 7 March) were not available, thus leaving 24 biweekly data points
164 at each station. We used this sampler dataset to validate the model procedure in a real setting (i.e.
165 with actual passive sampler data) and to verify if and how changes in wind patterns can
166 compromise the results. To this end, daily data on wind speed and direction for 2018 were obtained
167 from one monitoring station (M802, Havanastraat, Antwerpen) equipped with a weather station.
168 This allowed comparison of monthly and annual wind patterns.
169 All averages denote arithmetic means over a given time period, and the necessary data
170 processing and handling of missing data is described in detail in the Supplementary Information.
171 All data processing and analysis was performed in R 3.6.0. Wind roses were constructed from the
172 wind speed and direction data using the R package 'openair' **(27)**.

173 ## 2.3. Model development and cross validation

174 The extrapolation model seeks a relationship between the average NO_2 concentration measured
175 over a limited time period (T =2, 4, 6, 8 weeks) at a given location (the predictor variable X_i^R with
176 i = 1,.., N_R the number of stations), and the annual averaged NO_2 concentration from that same
177 location (Y_i^R). Three different models were tested: orthogonal regression, constant off-set and ratio
178 multiplication. The equations are provided in Sup. Mat. In the orthogonal regression model, the
179 slope a and intercept b were calculated using Deming regression using the 'mcreg' function in the
180 R package 'mcr' **(28)**, assuming equal uncertainties for X_i and Y_i.

For the two datasets analysed here, both the multi-week as well annual averaged NO_2 data are known. In real applications, these two data types will be available for the N_R reference locations, while the N_S sampler locations will have only multi-week data (Fig. 1c). We used the leave-one-out (LOO) approach to cross-validate the model approach. The goal of cross-validation is to test the model's ability to predict new data that was not used in estimating it, to give an insight on how the model will generalize to an independent dataset (i.e., a dataset at N_S sampler locations supplied by citizen science). To implement the LOO method and estimate the model error, we used the 'jackknife' function from the R package 'bootstrap' **(29)**.

Air quality directives require that the uncertainty of model approaches is explicitly quantified **(30,31)**, and associated model quality objectives are typically expressed as the relative uncertainty at the limit value of a given pollutant **(22)**. The EU air quality directive defines the model uncertainty as the maximum deviation between the measured and calculated concentrations for 90 % of monitoring points, and specifies that this uncertainty should be less than 30% for annual NO_2 values, defined at the limit value C_{lim} = 40 µg/m3 **(22)**. To verify whether our model meets the EU model quality objectives, we quantified the model uncertainty as the P90 value of the frequency distribution of residuals $\varepsilon_{i,p}^{R}(T, M)$ divided by C_{lim} (see Sup. Mat. for a definition of residuals and model errors).

3. Results

3.1. Spatial synchrony in NO_2 reference data

The central assumption of our extrapolation approach is that ambient NO_2 shows spatial synchrony when averaged over a multiple weeks, i.e. the relative concentration differences between locations within the study area remain stable in time. Figure 2a examines this idea of

spatial synchrony for NO_2 in the region of Flanders (Belgium). It shows a two-year time series from reference stations in the official monitoring network that are situated in different geographical locations and cover a range of emissions and concentrations levels (countryside, urban, industrial). Comparison of 4-week moving averages reveals considerable covariation in time between the stations (for clarity only 5 stations are displayed; a plot for all 67 available stations over the whole 8-yaer period shows the same behaviour – Fig. S1a). Spatial synchrony becomes even more apparent when the concentration at each site is normalised (as $X_i - \overline{X}_i$, where $\overline{X}_i$ is mean over the whole 8-year period at station i). The normalized concentrations at all 67 stations display a similar seasonal pattern and slowly decreasing trend with time (Fig. S1b).

Time series analysis shows that spatial synchrony becomes stronger as the averaging period becomes longer. To demonstrate this, we performed a pair-wise comparison of the time series of all stations **(32)**, after adopting a moving average that broadly encompasses the measurement period of passive samplers (1-50 days; Fig. S2). The average Pearson correlation across all station pairs rapidly increases from 1 day to 7 day averaging periods, as short term fluctuations are filtered away. Subsequently, the correlation increases more slowly (Fig. S2). Pairwise t-tests (in which the degrees of freedom were reduced for temporal autocorrelation with a lag period of 365 days) show that for an averaging period of 4-weeks, the correlation was significant for 98.5% of the pairs.

The dominant frequency component in the NO_2 data from the reference stations is the seasonal cycle. Figure 2b shows the evolution over eight years of the deviation between the inter-site mean of annual averages and 4-week averages, i.e, $\Delta = \langle Y_i^R \rangle - \langle X_{i,p}^R \rangle$, where the operator $\langle\ \rangle$ takes the arithmetic mean over all stations. The deviation Δ shows a clear seasonal cycle, where 4-week averaged NO_2 levels in summer are lower compared to the annual average, while they exceed the annual average in winter. The underlying mechanism is likely a combination of meteorology (more

227 stable atmospheric conditions with less dispersion) and increased emissions that favour higher
228 concentrations in winter months compared to the annual average, and lower concentrations in
229 summer **(33)**. The reference station that shows the least covariation with other stations is situated
230 at an oil refinery in the harbour of Antwerp (purple curve in Figure 2a). This is not unexpected, as
231 industries at different locations may show different temporal economic activity and associated
232 emissions patterns, thus diminishing covariation. Overall however, the temporal covariation of this
233 industrial station with urban and residential stations remains substantial, suggesting that region-
234 wide changes in meteorology remain an important driver at this industrial station.

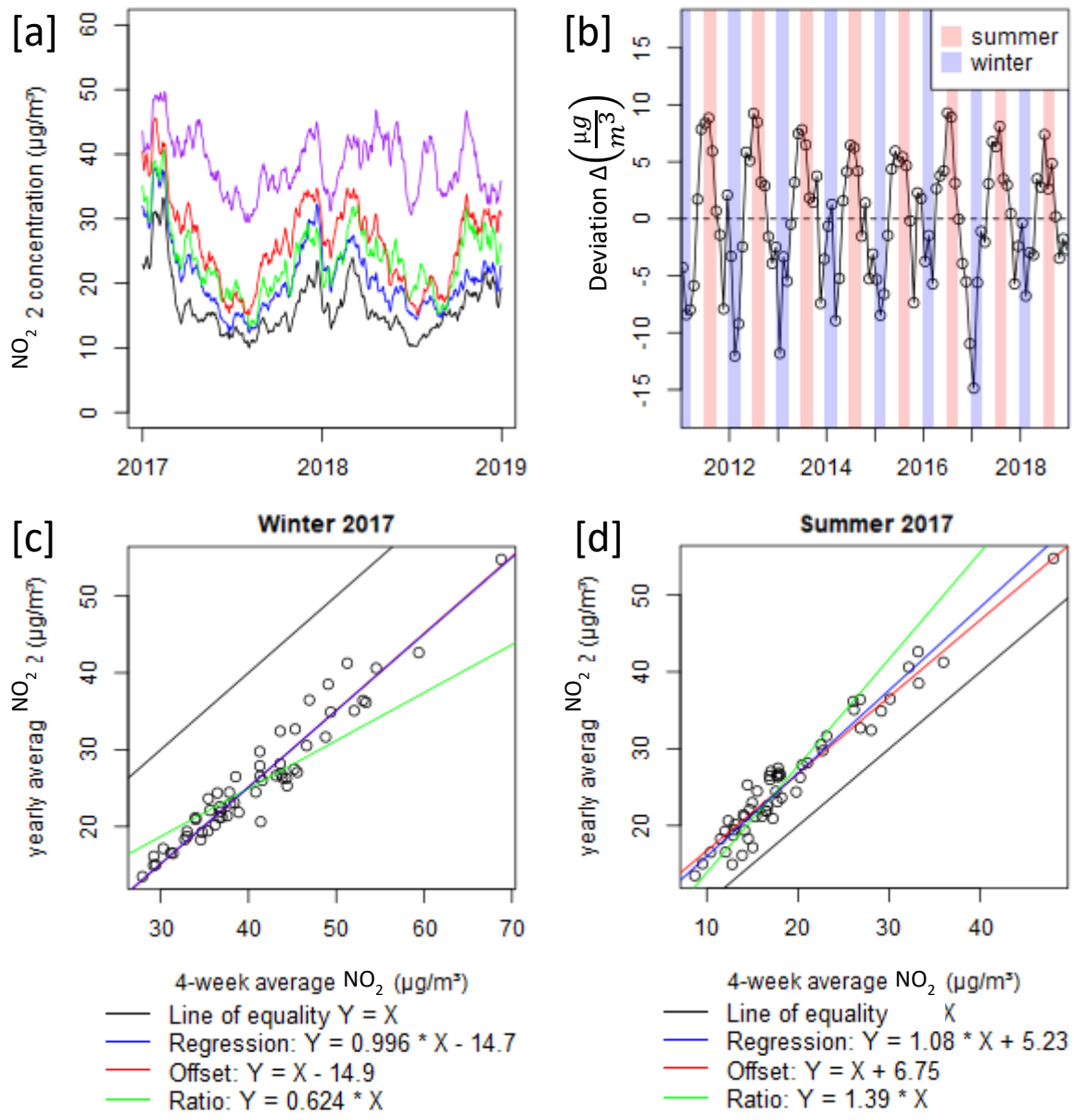

Figure 2. [a] NO_2 time series over 2 consecutive years at 5 stations selected from the reference monitoring network in Flanders. The curves denote the 4-week moving average of hourly NO_2 data. [b] The deviation between annual averaged NO_2 values and 4-week averages across the reference monitoring network over 8 consecutive years. The deviation $\Delta = \langle Y_i^R \rangle - \langle X_{i,p}^R \rangle$ takes the mean over all $N_R = 67$ stations in the network. Winter (Dec 21 to Mar 20) and summer (21 Jun

241 to 20 Sept) are shown in blue and red shading respectively. [c-d] Scatterplots of NO_2 data for NR
242 = 67 reference stations showing 4-week averages against annual averages for 2017 in [c] winter
243 (period 1 of 2017) and [d] summer (period 6 of 2017). Solid black lines denote 1:1 equality.
244 Coloured lines denote model fits.

245 ### 3.2. Model application to monitor data

246 The fact that the NO_2 data are spatially synchronous suggests that there could be a strong
247 correlation between multi-week averaged values X_i^R and annual averaged values Y_i^R for the
248 reference monitoring stations, regardless of the time of year. This is indeed the case, as illustrated
249 in Figure 2c-d for two separate 4-week periods, respectively in the winter and summer of 2017.
250 For all reference stations in the official monitoring network with available data (N_R = 57 stations),
251 the multi-week-average X_i^R is plotted versus the year-average Y_i^R over 2017. The X_i^R and Y_i^R
252 values show a high correlation (Pearson R: 0.962 in winter, 0.968 in summer) and the best fit of
253 the regression, offset and ratio models are shown. In winter the data fall below the 1:1 line
254 (negative Δ), while in summer one has the opposite situation (positive Δ). These examples are
255 highly representative for other periods in the 8 year data series. In all instances the data show a
256 clear linear relationship between multi-week-averaged and annual averaged NO_2 data (mean
257 Pearson R = 0.961 over all n=103 periods; range 0.88-0.99; Fig. S3).

258 Our analysis hence suggests that multi-week-averaged NO_2 data can be predictably extrapolated
259 to annual averaged values. So, what extrapolation model performs best? Table 1 depicts the overall
260 model performance for the three models (M = Regression, Offset and Ratio) as a function of the
261 averaging period (T = 2, 4, 6 or 8 weeks). Irrespective of the averaging period T, the Regression
262 model performs best (lowest RMSE), closely followed by the Offset model, while the Ratio model
263 gives a substantially higher RMSE in all cases. For all models, an increase in the length of the

averaging period T increases the model performance. The largest decrease in RMSE is realized when going from 2 to 4 weeks, whereas subsequent increases in T have a smaller effect, which is congruent with how the co-variation between stations depends upon the measurement period of passive samplers (Fig. S2).

Table 1. Summary of model-based extrapolation approach applied to the monitor dataset (upper part) and sampler dataset (lower part). A model-data comparison is performed for three different statistical models (Regression, Offset, Ratio) and for different averaging periods (T). The Root Mean Square Error (RMSE) and model uncertainty are tabulated. See section 1.2 in the Sup. Mat. for mathematical formulae.

Monitor dataset		**Regression**		**Offset**		**Ratio**	
Period T (weeks)	# periods	RMSE (µg/m³)	Uncertainty (%)	RMSE (µg/m³)	Uncertainty (%)	RMSE (µg/m³)	Uncertainty (%)
2	206	2.8	11.2	3.0	12.0	3.7	14.3
4	103	2.2	9.0	2.3	9.5	3.0	11.4
6	64	2.0	8.1	2.1	8.5	2.7	10.2
8	48	1.8	7.5	1.9	7.5	2.6	9.6

Sampler dataset		**Regression**		**Offset**		**Ratio**	
Period T (weeks)	# periods	RMSE (µg/m³)	Uncertainty (%)	RMSE (µg/m³)	Uncertainty (%)	RMSE (µg/m³)	Uncertainty (%)
2	24	3.5	13.1	3.5	13.7	4.3	16.2
4	11	2.8	11.0	2.9	11.7	3.7	14.1
6	8	2.4	9.4	2.5	10.9	3.3	13.2
8	5	2.2	9.6	2.3	9.7	2.9	11.1

Normal Q-Q plots reveal that the residuals from the Regression and Offset models are normally distributed, while the residuals of the Ratio model show tailing to the right (Fig. S4). Furthermore, analysis of variance (ANOVA) on the monitoring dataset shows that residuals do not depend on the averaging period T, the year or their interaction (P>0.9 for all associations). The model uncertainty for the three models ranges between 7.5% and 11.2%, well below the model quality objective of 30% as specified in the EU directive (Table 1).

3.3. Model application to sampler data

Until now our analysis has been exclusively based on NO_2 data obtained from reference monitoring stations. In real life however, the extrapolation procedure will principally target data obtained from passive sampler deployments. To verify whether this makes a difference, we investigated a data series of calibrated passive sampler data (N_S = 24 stations; 13 consecutive periods of 4 weeks over the year 2018). We implemented the Regression, Offset and Ratio models to calculate the predicted year-averaged values $Y_{i,p}^{S,model}(T,M)$ and compared these values with the actual year-averaged values $Y_i^{S,true}$ as derived from directly averaging the sampler data. Model results are highly similar to above (Table 1). Irrespective of the averaging period T, the Regression model performs best, closely followed by the Offset model. Model uncertainties are slightly higher than above (9.3-13.6%), but still fall well below the 30% model quality objective of the EU directive.

The model uncertainty in Table 1 is calculated from the model errors $\sigma_p^S(T,M)$, which require a year-long coverage of sampler data. In real-world applications however, sampler campaigns will only be conducted at a single instance, and not over a whole year. As a consequence, one cannot determine the model error $\sigma_p^S(T,M)$ directly. Still, when reference data are available, one can calculate the model error $\sigma_p^R(T,M)$ via the LOO approach, and then use the resulting value as an

297 estimate for $\sigma_p^S(T,M)$. Because passive samplers were co-located at reference stations, we can
298 calculate and compare the corresponding model errors $\sigma_p^R(T,M)$ and $\sigma_p^S(T,M)$ for each time
299 period of 4 weeks (residuals for all individual stations are shown in Fig. S5). Figure 3a shows that
300 the monitor-based and sampler-based model errors are of similar magnitude (ranging between 1
301 and 4 µg/m^3) and that they show the same temporal trend across the different measurements
302 periods. Moreover, there is an excellent linear relation between both model errors (Fig. 3b),
303 showing that $\sigma_p^R(T,M)$ indeed provides a good estimate of the sought-after model error $\sigma_p^S(T,M)$.
304 Consequently, the LOO approach based on monitor data provides an appropriate way to estimate
305 the model uncertainty when performing the model extrapolation on sampler data.
306
307

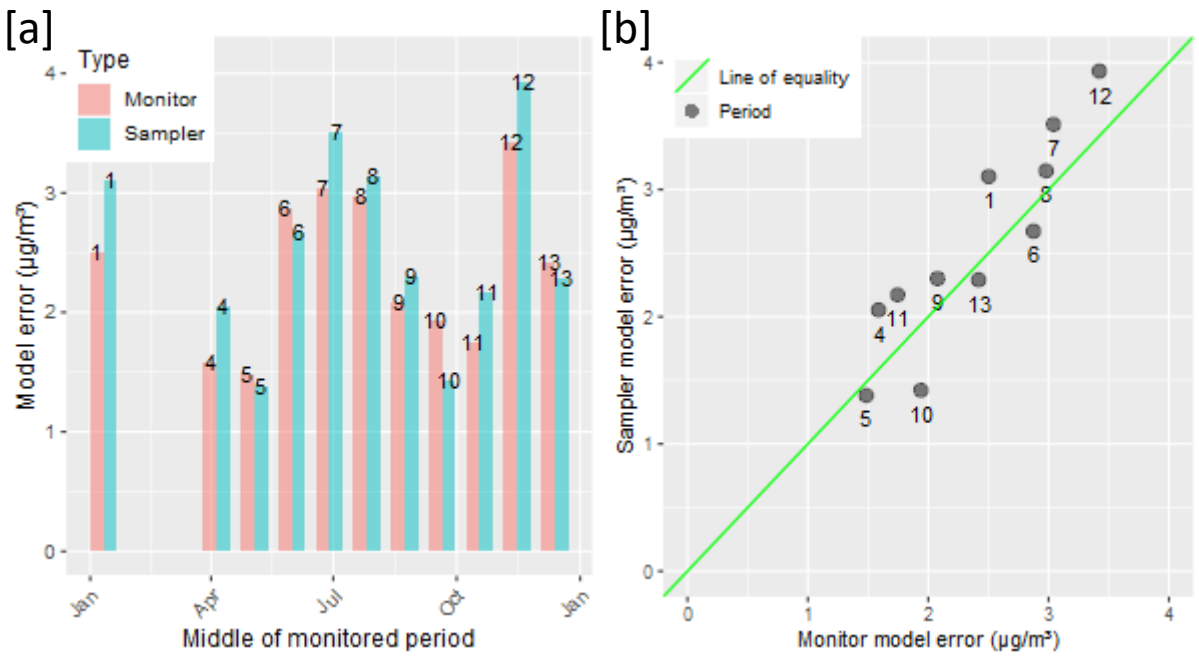

308
309 **Figure 3.** [a] Model errors from the orthogonal regression model as derived from both the sampler
310 dataset $\sigma_p^S(T,M)$ (green bars) and as derived from the monitor dataset by the LOO approach

311 $\sigma_p^R(T,M)$ (red bars). Values are plotted for each 4-week period in 2018. Data for periods 2 and 3
312 are missing. [b] Scatterplot of model errors as derived from sampler and monitor datasets. Solid
313 line denotes 1:1 equality. Numbers indicate the 4-week period.

314 ### 3.4. Wind effects

315 The above results demonstrate that multi-week NO_2 sampler data can be predictably extrapolated
316 to annual averaged values, and that this can be achieved with a relatively small uncertainty (< 11
317 % at T = 4 weeks). An important question is whether there are conditions where this model-based
318 extrapolation may induce large errors? In the 2018 passive sampling campaign, the largest residual
319 $\varepsilon_{i,p}^S(T,M)$ was obtained in period p = 12 at station R804 (M = Regression, T = 4 week). The
320 measured annual NO_2 concentration at this station was 15 µg/m³ higher than the model-predicted
321 value from this period (Fig. S5), and this residual was outside the 95% confidence interval of ±
322 5.6 µg/m³. A closer inspection of the positioning and wind dynamics provides an explanation for
323 this high deviation. Station R804 is situated immediately east of the R1 Ring Road, which is the
324 stretch of highway with the highest traffic intensity in Flanders (Fig. S6). Period 12 had an
325 unusually high proportion of easterly winds compared to the average wind pattern for 2018 (winds
326 from the southwest are dominant), which transport the high emissions from the highway away
327 from the monitoring station, thus explaining the observed underestimation of the annual averaged
328 NO_2 concentration. To explicitly account for such wind effects, more complex regression
329 approaches could be explored in future studies, which draw in data sources (such as wind direction,
330 speed) other than the NO_2 reference data used here in the extrapolation model.
331

4. Discussion

Recently, large-scale citizen science projects involving thousands of participants have generated extensive NO_2 datasets via passive samplers **(18–20,34)**. These datasets typically assess the averaged air quality over a limited time period (1-4 weeks), and could provide a valuable contribution to air quality policy, provided the data can be reliably upscaled to year-averaged values. Here, we have evaluated a procedure to reliably extrapolate the time-limited results of NO_2 passive samplers from multi-week to annual averaged values. Note that this approach implies an inversion of the traditional approach to air quality monitoring. Conventionally, the temporal variation of air quality is characterized in detail via reference stations, and subsequently, suitable spatial extrapolation occurs via geo-spatial interpolation, LUR or atmospheric dispersion models **(35)**. In the procedure developed here, one first characterizes the air quality in high spatial detail using citizen-based monitoring, and subsequently, one extrapolates these data in time to arrive at annual averages, which can then be used for compliance checking.

4.1. Spatial synchrony in NO_2 data

The central premise of our model procedure is that the air quality within the examined spatial domain shows spatial synchrony: when averaged over a suitably long period, sampling locations will preserve the spatial pattern in NO_2 concentrations, when assessed at different times. Early work with NO_2 passive samplers (2 week averages) already noted that urban sites with high pollution tend to remain polluted, and that sites rank in the same order during repeated surveys, although the absolute NO_2 concentrations may vary **(17)**. This temporal stability of spatial contrasts was corroborated by follow-up studies within metropolitan areas **(6,16, 25–26)**, but also appeared to hold for a larger region, like The Netherlands (**24**). Our statistical analysis of an 8-year NO_2 data series from the reference stations in the official monitoring network of Flanders

(Belgium) confirms the existence of strong spatial synchrony. More importantly, our analysis demonstrates that spatial synchrony increases with the period over which data are averaged (Fig. S2). Reference stations that are situated in different geographical locations and different emission regimes (countryside, urban, industrial) show a similar temporal variation, when short-term fluctuations are filtered away (Figure 2; Fig. S1). This indicates that the key drivers of longer-term NO_2 variation must act in a synchronous manner across the whole region of Flanders (which is 60 x 225 km in size and covers 13.700 km^2). Such drivers could include region-wide changes in economic activity that synchronize traffic NO_2 emissions, seasonal patterns in heating activity and household emissions, as well as seasonal variation in the structure of the atmospheric boundary layer, which could synchronize changes in dispersal between locations. Given this, we expect the spatial synchronicity to hold on a scale of a city, region or small country, but to break down on the larger scale of a large country or a continent.

Additionally, we find that spatial contrasts in pollutant concentrations remain stable over a time span of 8 years, which implies that either land use changes were not substantial enough to affect spatial synchronicity over this period, or alternatively, that land use changes went in a similar direction across the whole domain (i.e. increased urbanisation). This observation is of particular importance for the development of land-use regression (LUR) models, which provide a cost-effective approach for predicting the air quality at sites not covered by reference networks **(36,37)**. LUR models have been widely used in epidemiological studies and are often applied to time periods before (hindcasting) or after (forecasting) the period of air quality monitoring used in model development. The spatial synchrony as observed in our data justifies the temporal stability of LUR models, thus increasing their predictive power and reliability **(24–26)**.

4.2. Model-based extrapolation to annual NO_2 concentrations

Spatial synchrony of NO_2 data has an important additional advantage: it implies that there is a good correlation between multi-week-averaged NO_2 values and annual averaged values NO_2 for sampling stations within a wider region. This property has been occasionally employed to adjust passive sampler data for seasonal variability **(38)**, but its validity has not been systematically investigated. Here, we evaluated three different models to assess this correlation and estimated the model uncertainty associated with each model. The orthogonal regression model performs best overall, while the Ratio model performs the least well. It is not surprising that the orthogonal regression model performs best, as it is also the most complex model, of which the constant offset and ratio multiplication models are essentially special cases (forcing the slope to 1 or the offset to zero). However, it is remarkable that orthogonal regression model systematically shows a 1:1 slope and a non-zero offset, and as a result, the constant offset model almost performs equally well. This "offset" response is consistently observed throughout the 8 year long time series (Figure 2 c-d), and has been casually reported in passive sampler studies **(16,38)**. To explain this, one needs a process that affects countryside locations (low NO_2) and urban stations (high NO_2) in the same absolute manner, i.e., by subtraction or addition of a similar concentration difference. A simple seasonal change in the ventilation rate of the atmospheric boundary layer cannot account for this, as this would change the slope, but would not create an offset. One option is that seasonal weather patterns predominantly influence the regional background, with lower NO_2 values in summer compared to winter due to e.g. an expanded atmospheric boundary layer and increased photolysis of NO_2 in summer (Fig. 2b). This would affect all stations in a similar fashion, thus explaining the offset seen in the relation between multi-week-averaged and annual averaged NO_2 values (Figure 2c-d).

Our analysis demonstrates that the extrapolation from multi-week-averaged to annual averaged NO_2 values generally works well. Consequently, in large-scale campaigns with passive NO2 samplers (as done in citizen science projects), the extrapolation model will perform well for most locations. Still, there are a number of specific circumstances where one should be cautious for potentially biased results. Locations that are heavily influenced by variable industrial emissions need not be synchronous with other locations (Fig. 2a). Another point of attention are locations near a major pollution source (e.g. stations near highways) exposed to non-representative wind conditions. These locations may show strong underestimation or overestimation, depending on the direction of the wind (Fig. S6). More generally, the extrapolation of passive sampler data can be biased when the emission source contributions and meteorological conditions during the measurement period are not representative for the year over which the extrapolation occurs. Accordingly, one should scrutinize for deviations in meteo-conditions and source emissions, for example, when the traffic intensity deviates at a given location during the measurement period (e.g. due to road works).

4.3. Cost-efficient design of passive sampler campaigns

In addition to citizen science, low-cost passive sampler approaches are also widely employed by EPA's to identify localized hotspots or to complement the existing measurement network in a cost-efficient manner **(4,16)**. To meet with the data quality objectives for ambient air quality assessment, passive sampler campaigns are typically repeated throughout the year to ensure full time coverage (e.g. 12 consecutive monthly passive sampler campaigns). However, this is labour intensive, and so the capability to reliably extrapolate the data for a multi-week single to an annual averaged value – as proposed here - implies a substantial gain in terms of cost efficiency. For a one-off campaign, the extrapolation approach allows to increase the number of measurement

423 locations by a factor of 12. Alternatively, one could retain the sampling strategy with consecutive
424 multi-week campaigns, but select each time a different set of measurement locations. In both cases,
425 the resulting set of locations with annual NO_2 data will be expanded by a factor of 12 for the same
426 deployment effort (i.e. for the same amount of passive samplers analysed).

427 Our results provide some valuable guidelines for the optimal experimental design of passive
428 sampler campaigns. Table 1 shows the model uncertainty as a function of the measurement period
429 (T = 2, 4, 6, 8 weeks). The model uncertainty decreases for longer measurement periods, as
430 emissions and meteorology will show higher spatial synchrony when averaged over a longer period
431 (Fig. S2). When increasing T from 2 to 4 weeks, the model uncertainty substantially decreases, but
432 after that, the further improvement of the model uncertainty is marginal.

433 A critical concern with passive sampler measurements for longer periods is the saturation of the
434 samplers. For example, NO_2 diffusion tubes typically saturate after 4 weeks at urban traffic stations
435 with daily NO_2 values > 50 µg/m³. Deployment of these samplers over 2 weeks requires a similar
436 effort than deployment over 4 weeks (both require one single campaign), but due to the risk of
437 saturation, deployment over 6 or 8 weeks necessitates a doubling of the effort (2 consecutive
438 campaigns are needed). Accordingly, 4-week deployment seems to be an optimal balance
439 (enlarging T to reduce model uncertainty while avoiding the risk of saturation).

440 ### 4.4. Compliance with EU legislation

441 The spatially dense datasets resulting from large-scale citizen science projects complement the
442 data resulting from the sparse official networks of reference monitor stations. But to what extent
443 do they comply with existing legislation? Currently, the EU Directive on ambient air quality and
444 cleaner air for Europe **(22)** allows for two types of data in addition to data from reference stations:
445 indicative measurements and model estimates. For indicative measurements, the EU Directive

446 requires a minimum of time coverage of 14% (i.e., at least one measurement a week at random,
447 evenly distributed over the year, or eight weeks evenly distributed over the year). Data collected
448 within citizen science projects (e.g. in a single 4-week campaign) typically do not meet this
449 criterion, and so they cannot qualify as indicative measurements.

450 In essence, the annual averaged NO_2 data derived from our extrapolation procedure are model
451 estimates. However, the legal status of these data is uncertain, because it is not clear whether they
452 comply with the strict definition of "model estimates" as described in the EU Directive. This is
453 because the EU Directive currently adopts a different view on the usage of models, which does not
454 include the model approach adopted here. When the EU Directive considers "model approaches",
455 the underlying idea is that datasets are available with high temporal resolution and low spatial
456 resolution (as generated by reference networks), and that geo-spatial, LUR or transport models are
457 used to perform spatial interpolation (see article 6, paragraph 2 in the EU Directive :"provide
458 adequate information on the spatial distribution"). Here however, we tackle the opposite problem:
459 citizen science typically generates datasets that have high spatial resolution (thousands of
460 participants) but low temporal coverage (only a few weeks). As a consequence, one needs a model
461 approach that performs temporal extrapolation: passive sampler data collected over a measuring
462 period of weeks need to be extrapolated to annual averaged values.

463 The emergence of large-scale air quality datasets from citizen science, as discussed here, is a
464 recent phenomenon and hence it is not surprising that the existing legislation does not properly
465 accommodate these particular data types. Future legal guidelines may include additional data types
466 and model protocols, provided they can demonstrate suitable compliance with quality standards.
467 Our results here demonstrate that citizen derived annual averaged NO_2 data do meet the stringent
468 data quality criteria imposed the current EU directive, which requires a maximal model uncertainty

of 30%. Based on the deviation for a 4-week period extrapolation using the orthogonal regression in **Table 1** (2.2 – 2.8 µg/m³), the model uncertainty at 40 µg/m³ (the current WHO and EU limit for annual averages) is 9-11%, which is well below the quality criterion of 30% imposed by the EU Directive.

In summary, short term but spatially extensive measurements campaigns through citizen science provide an important new data resource, complementing data from official reference networks. However, the existing air quality legislation is currently not well adapted to accommodate these spatially distributed data with short-term coverage. Our results demonstrate that these data can form a powerful resource for policy support. Foremost, air pollutants like NO_2 reveal spatial synchrony across broad regions, and one can take advantage of this property to develop reliable statistical model extrapolation that map short-term data into annual averages. Longer-term deployment of passive samplers reduces model uncertainty, and allows the resulting annual NO_2 values to meet the stringent data standards for air quality compliance. Accordingly, we propose that future air quality legislation should explicitly consider the existence and use of these data types and model approaches, and in this way, citizen-derived data could directly feed into air quality policy. As it happens, the prospect of producing data that are useful to society and policy is an important motivation for citizens to participate in citizen science projects **(18)**.

Supporting information

The Supporting Information is available free of charge at ?? and consists of a single text file (PDF) that contains on

- Supplementary Methods: Data processing and handling of missing data
- Supplementary Methods: Model development
- Supplementary Methods: Model application on monitoring data

- Supplementary Methods: Model application on passive sampler dat
- Supplementary Figures S1 to S6

Author contributions

FJRM conceived the idea of the model approach. DCS performed data analysis model calculations with input of JV. FJRM wrote the manuscript with contributions of all authors. All authors have given approval to the final version of the manuscript.

The authors declare no competing financial interest.

Acknowledgements

This work was supported by funding for the citizen science project CurieuzeNeuzen Vlaanderen. We thank Prof. R. Blust at University of Antwerp, M. Naert at the newspaper De Standaard and Mr. M. Van Peteghem at Vlaamse Milieumaatschappij for enabling the CurieuzeNeuzen project, and all 20.000 citizens for data collection. We thank Huib Huyse for help with the data collection design and Joris van den Bossche for input at an early stage of model development.

5. References

(1) WHO. *Ambient Air Pollution: A Global Assessment of Exposure and Burden of Disease*; Geneva, Switzerland, 2016.

(2) Gulia, S.; Shiva Nagendra, S. M.; Khare, M.; Khanna, I. Urban Air Quality Management-A Review. *Atmos. Pollut. Res.* **2014**, *6* (2), 286–304. https://doi.org/10.5094/apr.2015.033.

(3) Vardoulakis, S.; Solazzo, E.; Lumbreras, J. Intra-Urban and Street Scale Variability of BTEX, NO2 and O3 in Birmingham, UK: Implications for Exposure Assessment. *Atmos. Environ.* **2011**, *45* (29), 5069–

5078. https://doi.org/10.1016/J.ATMOSENV.2011.06.038.

(4) Cyrys, J.; Eeftens, M.; Heinrich, J.; Ampe, C.; Armengaud, A.; Beelen, R.; Bellander, T.; Beregszászi, T.; Birk, M.; Cesaroni, G.; Cirach, M.; de Hoogh, K.; De Nazelle, A.; de Vocht, F.; Declercq, C.; Ddel, A.; Dimakopoulou, K.; Eriksen, K. T; Galassi, C.; Grauleviiene; R.; Grivas, G.; Gruzieva, O.; Gustafsson, A. H.; Hoffmann, B.; Iakovides, M.; Ineichen, A.; Krämer, U.; Lanki, T.; Lozano, P.; Madsen, C.; Meliefste, K.; Modig, L.; Mölter, A.; Mosler, G.; Nieuwenhuijsen, M.; Nonnemacher, M.; Oldenwening, M.; Peters, A.; Pontet, S.; Probst-Hensch, N.; Quass, U.; Raaschou-Nielsen, O.; Ranzi, A.; Sugiri, D.; Stephanou, E. G.; Taimisto, P.; Tsai, M.; Vaskövi, É.; Villani, S.; Wang, M.; Brunekreef, B.; Hoek, G. Variation of NO_2 and NO_x concentrations between and within 36 European Study Areas: Results from the ESCAPE Study. *Atmos. Environ.* **2012**, *62* (2), 374–390. https://doi.org/10.1016/j.atmosenv.2012.07.080.

(5) Wu, H.; Reis, S.; Lin, C.; Beverland, I. J.; Heal, M. R. Identifying Drivers for the Intra-Urban Spatial Variability of Airborne Particulate Matter Components and Their Interrelationships. *Atmos. Environ.* **2015**, *112*, 306–316. https://doi.org/10.1016/J.ATMOSENV.2015.04.059.

(6) Lin, C.; Feng, X.; Heal, M. R. Temporal Persistence of Intra-Urban Spatial Contrasts in Ambient NO2, O3 and Ox in Edinburgh, UK. *Atmos. Pollut. Res.* **2016**, *7* (4), 734–741. https://doi.org/10.1016/j.apr.2016.03.008.

(7) Vardoulakis, S.; Gonzalez-Flesca, N.; Fisher, B. E. A.; Pericleous, K. Spatial Variability of Air Pollution in the Vicinity of a Permanent Monitoring Station in Central Paris. *Atmos. Environ.* **2005**, *39* (15 SPEC. ISS.), 2725–2736. https://doi.org/10.1016/j.atmosenv.2004.05.067.

(8) Santiago, J. L.; Martín, F.; Martilli, A. A Computational Fluid Dynamic Modelling Approach to Assess the Representativeness of Urban Monitoring Stations. *Sci. Total Environ.* **2013**, *454–455*, 61–72.

https://doi.org/10.1016/j.scitotenv.2013.02.068.

(9) Yatkin, S.; Gerboles, M.; Belis, C. A.; Karagulian, F.; Lagler, F.; Barbiere, M.; Borowiak, A. Representativeness of an Air Quality Monitoring Station for PM2.5 and Source Apportionment over a Small Urban Domain. *Atmos. Pollut. Res.* **2019**. https://doi.org/10.1016/j.apr.2019.10.004.

(10) Hafkenscheid, T.; Fromage-Marriette, A.; Goelen, E.; Hangartner, M.; Pfeffer, U.; Plaisance, H.; De Santis, F.; Saunders, K.; Swaans, W.; Tang, S.; Targa , J.; Gerboles, M. *Review of the Application of Diffusive Samplers for the Measurement of Nitrogen Dioxide in Ambient Air in the European Union*; EUR - Scientific and Technical Research Reports. 2009. ISBN: 978-92-79-12052-7

(11) Kracht, O.; Santiago, J. L.; Martin, F.; Piersanti, A.; Cremona, G.; Vitali, L.; Delaney, K.; Basu, B.; Ghosh, B.; Spangl, W.; Brendle C.; Latikka J.; Kousa A.; Pärjälä E.; Meretoja M.; Malherbe L.; Letinois L.; Beauchamp M.; Lenartz F.; Hutsemekers V.; Nguyen L.; Hoogerbrugge R.; Eneroth K.; Silvergren S.; Hooyberghs H.; Viaene P.; Maiheu B.; Janssen S.; Roet D.; Gerboles M. *Spatial Representativeness of Air Quality Monitoring Sites - Outcomes of the FAIRMODE/AQUILA Intercomparison Exercise*; 2017. https://doi.org/10.2760/60611.

(12) Palmes, E. D.; Gunnison, A. F.; Dimattio, J.; Tomczyk, C. Personal Sampler for Nitrogen Dioxide. *Am. Ind. Hyg. Assoc. J.* **1976**. https://doi.org/10.1080/0002889768507522.

(13) Gerboles, M.; Buzica, D.; Amantini, L.; Lagler, F.; Hafkenscheid, T. Feasibility Study of Preparation and Certification of Reference Materials for Nitrogen Dioxide and Sulfur Dioxide in Diffusive Samplers. *J. Environ. Monit.* **2006**, *8* (1), 174–182. https://doi.org/10.1039/b509559j.

(14) Cape, J. N. The Use of Passive Diffusion Tubes for Measuring Concentrations of Nitrogen Dioxide in Air. *Crit. Rev. Anal. Chem.* **2009**, *39* (4), 289–310. https://doi.org/10.1080/10408340903001375.

(15) Weissert, L. F. F.; Salmond, J. A. A.; Miskell, G.; Alavi-Shoshtari, M.; Williams, D. E. E. Development

of a Microscale Land Use Regression Model for Predicting NO_2 concentrations at a Heavy Trafficked Suburban Area in Auckland, NZ. *Sci. Total Environ.* **2018**, *619–620*, 112–119. https://doi.org/10.1016/j.scitotenv.2017.11.028.

(16) Caballero, S.; Esclapez, R.; Galindo, N.; Mantilla, E.; Crespo, J. Use of a Passive Sampling Network for the Determination of Urban NO 2 Spatiotemporal Variations. *Atmos. Environ.* **2012**, *63*, 148–155. https://doi.org/10.1016/j.atmosenv.2012.08.071.

(17) Lebret, E.; Briggs, D.; Van Reeuwijk, H.; Fischer, P.; Smallbone, K.; Harssema, H.; Kriz, B.; Gorynski, P.; Elliott, P. Small Area Variations in Ambient NO2 Concentrations in Four European Areas. *Atmos. Environ.* **2000**, *34* (2), 177–185. https://doi.org/10.1016/S1352-2310(99)00292-7.

(18) Van Brussel, S.; Huyse, H. Citizen Science on Speed? Realising the Triple Objective of Scientific Rigour, Policy Influence and Deep Citizen Engagement in a Large-Scale Citizen Science Project on Ambient Air Quality in Antwerp. *J. Environ. Plan. Manag.* **2018**, No. February, 1–18. https://doi.org/10.1080/09640568.2018.1428183.

(19) Haklay, M.; Eleta, I. On the Front Line of Community-Led Air Quality Monitoring. In *Integrating Human Health into Urban and Transport Planning: A Framework*; 2018. https://doi.org/10.1007/978-3-319-74983-9_27.

(20) Irwin, A. No PhDs Needed: How Citizen Science Is Transforming Research. *Nature*. 2018. https://doi.org/10.1038/d41586-018-07106-5.

(21) Heal, M. R.; Laxen, D. P. H.; Marner, B. B. Biases in the Measurement of Ambient Nitrogen Dioxide (NO2) by Palmes Passive Diffusion Tube: A Review of Current Understanding. *Atmosphere (Basel).* **2019**, *10* (7), 357. https://doi.org/10.3390/atmos10070357.

(22) European Commission. Directive 2008/50/EC of the European Parliament and of the Council of 21

May 2008 on Ambient Air Quality and Cleaner Air for Europe. Brussels, Belgium 2008.

(23) World Health Organization. WHO Air quality guidelines for particulate matter, ozone, nitrogen dioxide and sulfur dioxide: global update 2005: summary of risk assessment. 2006 https://apps.who.int/iris/handle/10665/69477

(24) Eeftens, M.; Beelen, R.; Fischer, P.; Brunekreef, B.; Meliefste, K.; Hoek, G. Stability of Measured and Modelled Spatial Contrasts in NO2 over Time. *Occup. Environ. Med.* **2011**, *68* (10), 765–770. https://doi.org/10.1136/oem.2010.061135.

(25) Cesaroni, G.; Porta, D.; Badaloni, C.; Stafoggia, M.; Eeftens, M.; Meliefste, K.; Forastiere, F. Nitrogen Dioxide Levels Estimated from Land Use Regression Models Several Years Apart and Association with Mortality in a Large Cohort Study. *Environ. Heal.* **2012**, *11* (1), 48. https://doi.org/10.1186/1476-069X-11-48.

(26) Wang, R.; Henderson, S. B.; Sbihi, H.; Allen, R. W.; Brauer, M. Temporal Stability of Land Use Regression Models for Traffic-Related Air Pollution. *Atmos. Environ.* **2013**, *64*, 312–319. https://doi.org/10.1016/j.atmosenv.2012.09.056.

(27) Carslaw, D. C.; Ropkins, K. Openair - an R Package for Air Quality Data Analysis. *Environ. Model. Softw.* **2012**, *27–28*, 52–61.

(28) Manuilova, E.; Schuetzenmeister, A.; Model, F. Mcr: Method Comparison Regression. R Package Version 1.2.1. 2014.

(29) Tibshirani, R.; Leisch, F. Bootstrap: Functions for the Book “An Introduction to the Bootstrap”. R Package Version 2019.6. 2019.

(30) EEA. The Application of Models under the European Union's Air Quality Directive: a Technical

Reference Guide. Technical report No 10/2011. ISBN: 978-92-9213-223-1, 2011. https://www.eea.europa.eu/publications/fairmode

(31) Thunis, P.; Pederzoli, A.; Pernigotti, D. Performance Criteria to Evaluate Air Quality Modeling Applications. *Atmos. Environ.* **2012**, *59*, 476–482. https://doi.org/10.1016/j.atmosenv.2012.05.043.

(32) Pyper, B. J.; Peterman, R. M. Comparison of Methods to Account for Autocorrelation in Correlation Analyses of Fish Data. **1998**, *2140*, 2127–2140.

(33) Henschel, S.; Le Tertre, A.; Atkinson, R. W.; Querol, X.; Pandolfi, M.; Zeka, A.; Haluza, D.; Analitis, A.; Katsouyanni, K.; Bouland, C.; Pascal, M.; Medina, S.; Goodman, P. Trends of Nitrogen Oxides in Ambient Air in Nine European Cities between 1999 and 2010. *Atmos. Environ.* **2015**, *117*, 234–241. https://doi.org/10.1016/j.atmosenv.2015.07.013.

(34) Greenpeace. Mijn Lucht, Mijn School. Onderzoek naar luchtvervuiling in 222 Belgische scholen; 2018. https://www.greenpeace.org/belgium/nl/rapport/1399/mijn-lucht-mijn-school/

(35) Thunis, P.; Miranda, A.; Baldasano, J. M.; Blond, N.; Douros, J.; Graff, A.; Janssen, S.; Juda-Rezler, K.; Karvosenoja, N.; Maffeis, G.; Martilli, A.; Rasoloharimahefa, M.; Real, E.; Viaene, P.; Volta, M.; White, Les L.E. Overview of Current Regional and Local Scale Air Quality Modelling Practices: Assessment and Planning Tools in the EU. *Environ. Sci. Policy* **2016**, *65*, 13–21. https://doi.org/10.1016/j.envsci.2016.03.013.

(36) Henderson, S. B.; Beckerman, B.; Jerrett, M.; Brauer, M. Application of Land Use Regression to Estimate Long-Term Concentrations of Traffic-Related Nitrogen Oxides and Fine Particulate Matter. *Environ. Sci. Technol.* **2007**, *41* (7), 2422–2428. https://doi.org/10.1021/es0606780.

(37) Hoek, G.; Beelen, R.; de Hoogh, K.; Vienneau, D.; Gulliver, J.; Fischer, P.; Briggs, D. A Review of Land-

Use Regression Models to Assess Spatial Variation of Outdoor Air Pollution. *Atmos. Environ.* **2008**, *42* (33), 7561–7578. https://doi.org/10.1016/j.atmosenv.2008.05.057.

(38) Lewné, M.; Cyrys, J.; Meliefste, K.; Hoek, G.; Brauer, M.; Fischer, P.; Gehring, U.; Heinrich, J.; Brunekreef, B.; Bellander, T. Spatial Variation in Nitrogen Dioxide in Three European Areas. *Sci. Total Environ.* **2004**, *332* (1–3), 217–230. https://doi.org/10.1016/j.scitotenv.2004.04.014.

Supplementary Material

Using large-scale NO_2 data from citizen science for air quality compliance and policy support

De Craemer Sam[1,2], Vercauteren Jordy[3], Fierens Frans[4], Wouter Lefebvre[2], Meysman J.R. Filip[1,5,]*

[1] Department of Biology, University of Antwerp, Universiteitsplein 1, B-2610 Wilrijk, Belgium

[2] VITO, Boeretang 200, 2400 Mol, Belgium

[3] Vlaamse Milieumaatschappij, Kronenburgstraat 45, 2000 Antwerpen, Belgium

[4] Belgian Interregional Environment Agency, Gaucheretstraat 92-94, 1030 Brussels, Belgium

[5] Department of Biotechnology, Delft University of Technology, Van der Maasweg 9, 2629 HZ Delft, The Netherlands

1. Supplementary methods

1.1. Data processing and handling of missing data

For the "monitor" dataset, day-averaged NO_2 values were calculated from hourly monitor data at each individual reference station. Day-averaged values were coded as missing when less than 75% of the hourly data were available. Time-averaged X_i^R values were calculated from day-averaged data for distinct time periods (T = 2, 4, 6 and 8 weeks) and were coded as missing when <75% of the daily data was present. Year-averaged $Y_i^{R,true}$ values were also calculated from day-averaged data and were coded as missing when <90% of the daily data were available.

For the "sampler" dataset, bi-weekly sampler data were either used as such (T = 2 weeks), or averaged over longer time periods (T = 4, 6 and 8 weeks). X_j^S values were set as missing when one or more of the bi-weekly measurements were missing. Yearly averaged $Y_j^{S,true}$ values were coded as missing when <75% of the data were available (not counting periods 4 and 5 for which no sampler data were available).

1.2 Model development

For the 67 stations in the "monitor" dataset, we used 3 different models to describe the relation between monthly-averaged values X_i^R and yearly-averaged values Y_i^R for a subset of stations, and then applied these models to calculate the yearly-averaged concentrations $Y_j^{R,\ model}$ for an independent subset of stations. We subsequently compared the model estimates $Y_j^{R,\ model}$ to the "true" yearly-averaged values $Y_j^{R,\ true}$ that were obtained by direct averaging of the monitoring data. Furthermore, we determined the model error and uncertainty associated with each regression approach and investigated the impact of the specific time averaging window (T = 2, 4, 6 and 8 weeks) used for the independent variables X_i^R.

For each of the 24 stations in the "sampler" dataset, we extrapolated the sampler data X_j^S from different sampling periods to yearly-averaged Y_j^S . To this end, we first performed a regression model between the biweekly-averaged X_i^R values and yearly-averaged Y_i^R values for the 24 reference monitoring stations at which the samplers were co-located. We then applied this model to the measured sampler concentrations X_j^S to arrive at model estimates $Y_j^{S,model}$. Because we have a full annual cycle of passive sampler measurements, we can compare the model estimates $Y_j^{S,model}$ to the true yearly averaged sampler data $Y_j^{S,\ true}$. Subsequently, we investigated the largest deviations between modeled $Y_j^{S,\ model}$ and measured $Y_j^{S,\ true}$ yearly averages.

Three different models were tested: orthogonal regression, constant off-set and ratio multiplication:

$$Y_i = a * X_i + b \quad (1)$$

$$Y_i = X_i + c \quad (2)$$

$$Y_i = r * X_i \quad (3)$$

In the orthogonal regression model, the slope a and intercept b were calculated using Deming regression using the 'mcreg' function in the R package 'mcr' **(28)**, assuming equal uncertainties for X_i and Y_i. The parameter c in the constant off-set model was determined as the mean of all individual offsets

$$c = \frac{1}{n}\sum_{i=1}^{n}(Y_i - X_i) \tag{4}$$

In the ratio multiplication model, the parameter r was determined as the mean of the individual ratios for all stations

$$r = \frac{1}{n}\sum_{i=1}^{n}\left(\frac{Y_i}{X_i}\right) \tag{5}$$

1.3 Model application on monitoring data

We used the above 3 models (M = regression, offset, ratio) to describe the relation between the multi-week-averages $X_{i,p}^{R}$ (averaging period length T = 2, 4, 6 or 8 weeks) and the associated annual averaged values $Y_{i,p}^{R}$. The subscript i denotes the specific station (i = 1..N_R), while p denotes the specific time period (p=1..n; the total time series is covered by n periods of length T). We used the jackknife or leave-one-out (LOO) method to estimate the model error, implementing the 'jackknife' function from the R package 'bootstrap' **(29)**. For a given station i and a given period p, we predicted first the annual average $Y_{j,p}^{R,\ model}$ by implementing a given model to the data for all other N_p^R -1 stations (hence excluding station i). The residual is then defined as the difference between the model value and the true value as directly calculated from the data series

$$\varepsilon_{i,p}^{R}(T,M) = Y_{i,p}^{R,model}(T,M) - Y_i^{R,true} \tag{6}$$

The model error for the period p is then calculated as the Root Mean Square Error over all stations, i.e., the standard deviation of the residuals

$$\sigma_p^R(T,M) = \sqrt{\frac{1}{N_R}\sum_i \varepsilon_{i,p}^{R}(T,M)^2} \tag{7}$$

The model error is dependent upon a specific period p, a specific model M and a specific averaging period length T. We can subsequently define the *overall model error* as the Root Mean Square Error over all stations for all periods

$$\sigma^R(T,M) = \sqrt{\frac{1}{nN_R}\sum_p\sum_i \varepsilon_{ip}^R(T,M)^2} \quad (8)$$

This way, we can compare the model errors for different models M and different averaging period lengths T.

1.4 Model application on passive sampler data

The 3 models (M = regression, offset, ratio) were applied in a similar way as above. The only difference is that models are derived from an independent dataset (i.e., the X_i^R and Y_i^R at the monitoring stations where samplers are co-located), and so we do not need to use the leave-one-out (LOO) method. The residual is now directly defined as the difference between the model estimate and the true value at the sampler station as calculated from the sampler data series

$$\varepsilon_{i,p}^S(T,M) = Y_{i,p}^{S,model}(T,M) - Y_i^{S,true} \quad (9)$$

The overall model error becomes

$$\sigma^S(T,M) = \sqrt{\frac{1}{nN_S}\sum_p\sum_i \varepsilon_{ip}^S(T,M)^2} \quad (10)$$

2. Supplementary figures

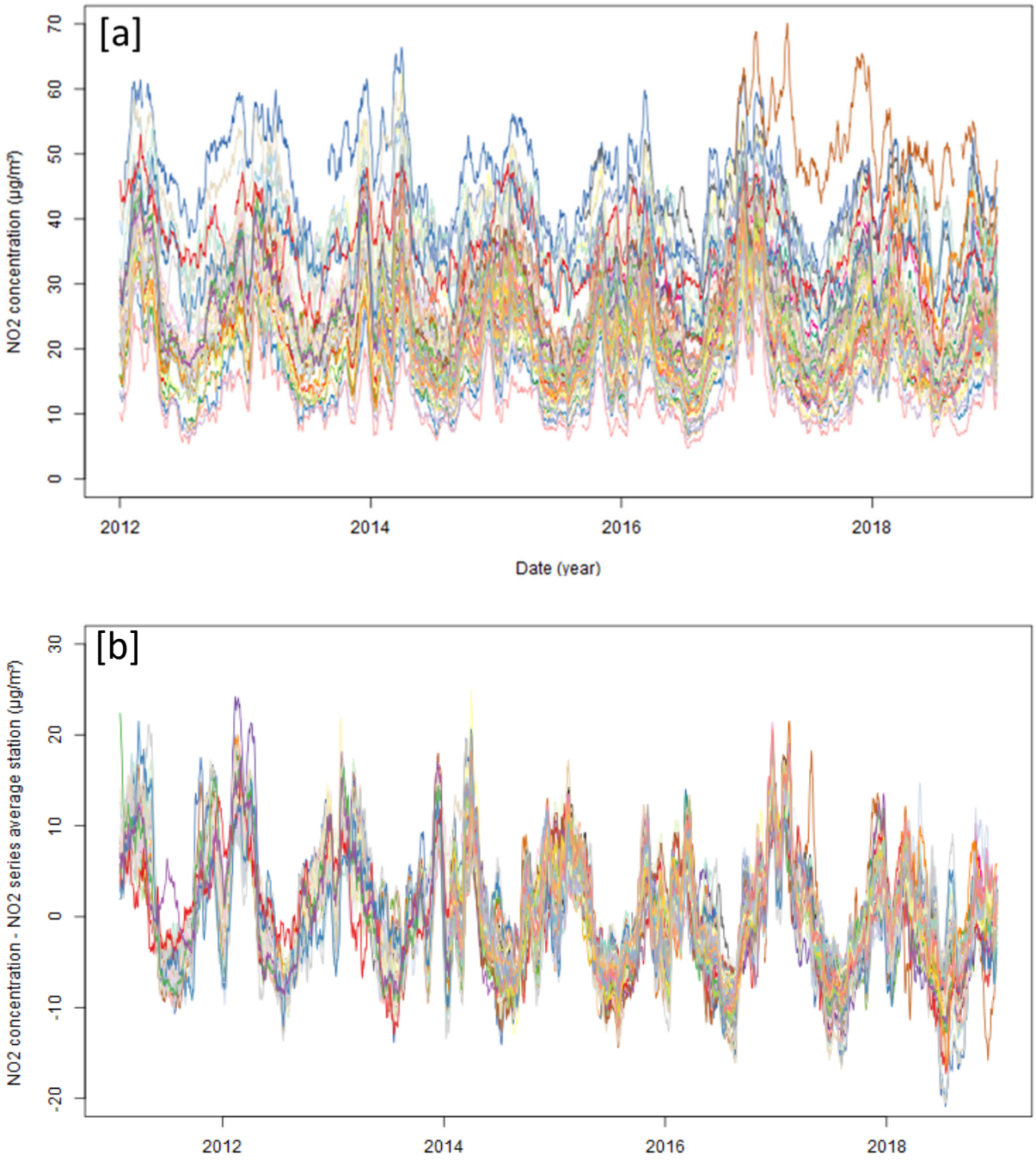

Figure S1. *Temporal variation in NO_2 concentration for the stations in the official reference monitoring network in Flanders (Belgium). The coloured lines denote 4-week moving averages of hourly NO_2 data for individual stations. [a] NO_2 time series over 8 consecutive years at all 67 stations of the monitoring network. [b] The same time series, but normalized. For each station, the mean NO_2 concentration over the 8 year period is subtracted. All 67 stations display a similar seasonal pattern and slowly decreasing trend with time.*

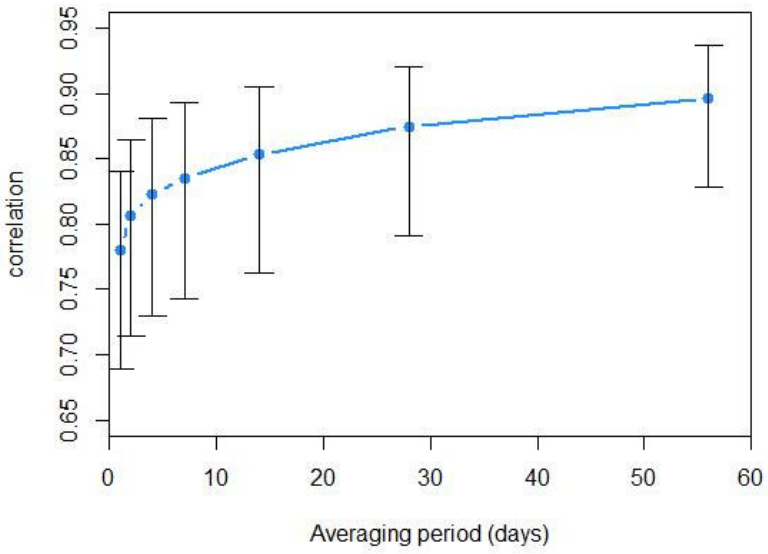

Figure S2. *Time series analysis of the NO_2 time series for all 67 stations in the official reference monitoring in Flanders (Belgium). A pair-wise comparison of the time series of the stations is performed after application of a moving averaging filter (we restricted the analysis to station pairs that had at least 13 months of overlapping data). The average Pearson correlation R across all 1934 station pairs is plotted as a function of the moving averaging period. The time series become more correlated as the averaging period increases.*

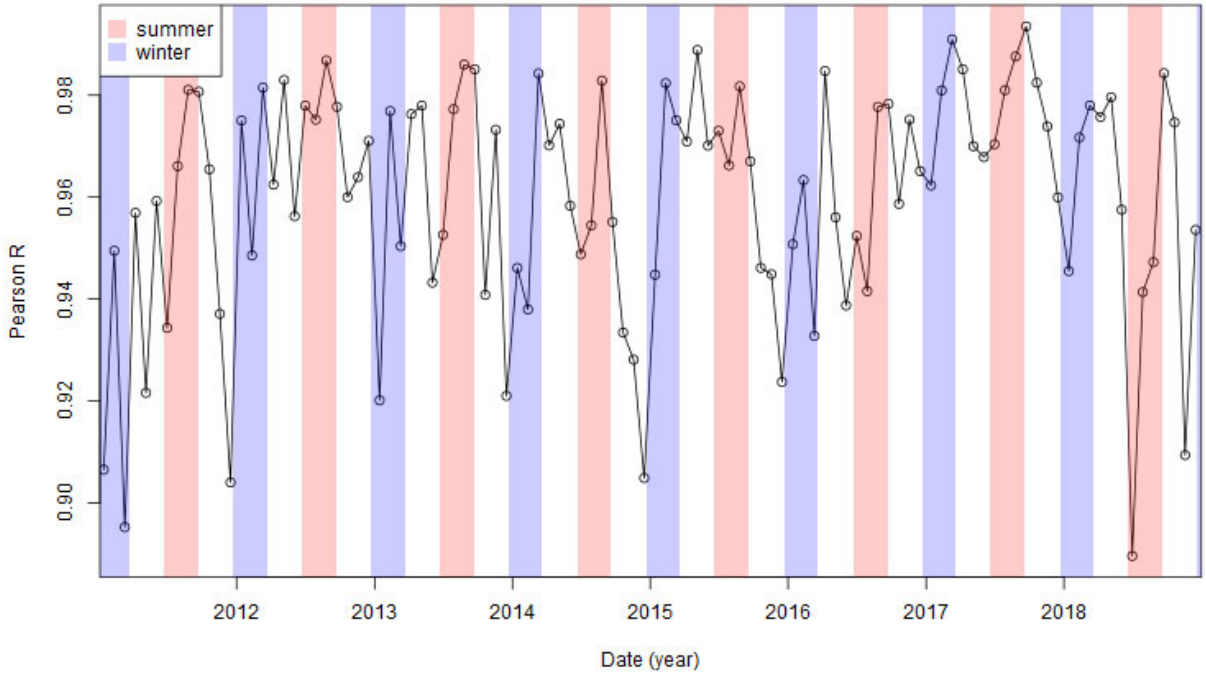

Figure S3. *Temporal variation in the Pearson R correlation between monthly and yearly NO_2 data from the official reference monitoring in Flanders (Belgium). The correlation is systematically high (>90%). The data are displayed per 4 week period. Winter (December 21 to March 20) and summer (June 21 to September 20) periods are shown in respectively blue and red shading.*

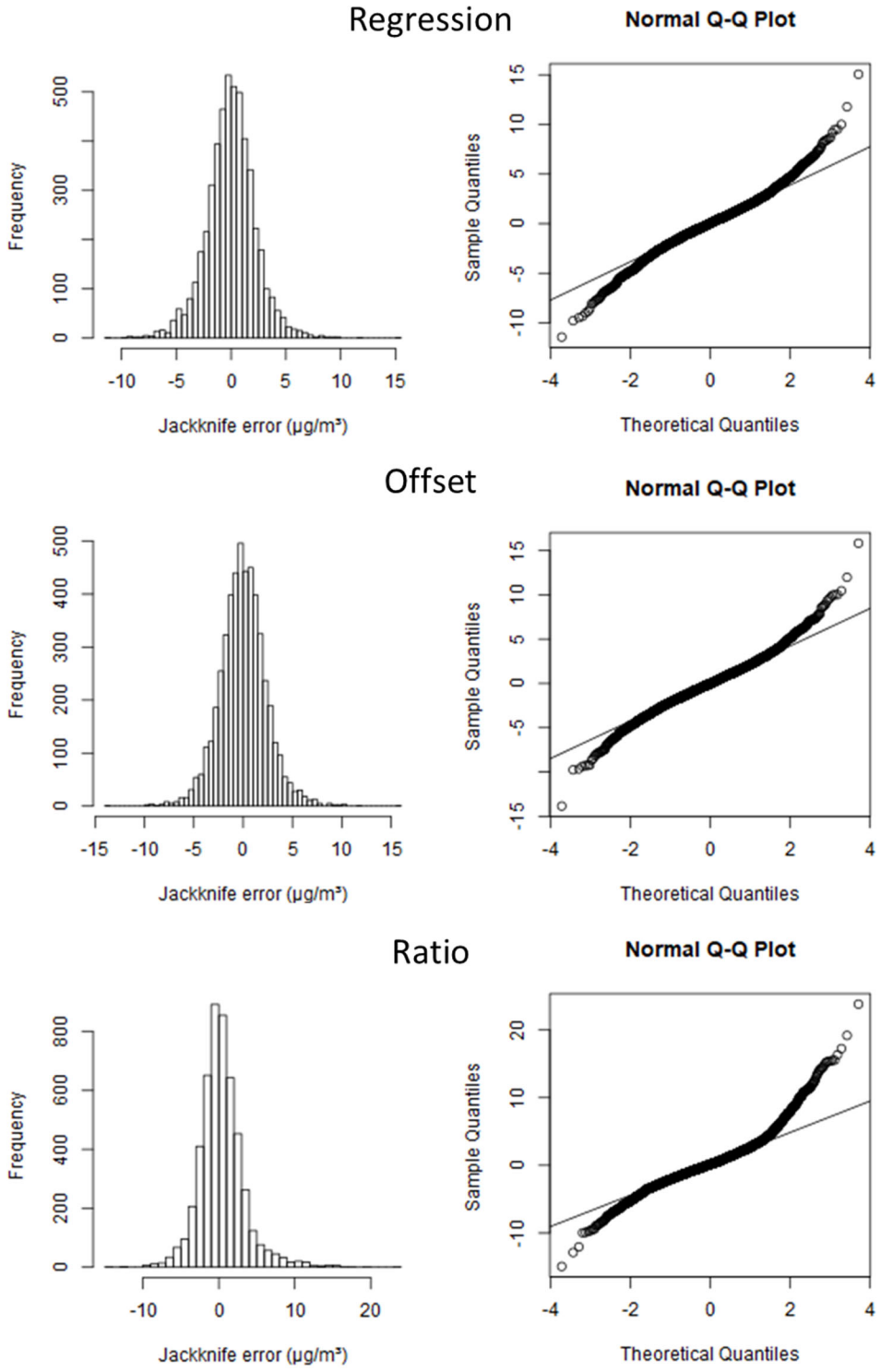

Figure S4. *Histogram and Q-Q plots of residuals obtained by analysis of the monitor dataset. Residuals (Jackknife errors) as determined by Eq (6) in the main text through application of the Leave-One-Out procedure to model extrapolation from the 4-week periods to year averaged NO_2 values. The results are displayed for three different models (regression, offset and ratio) are displayed.*

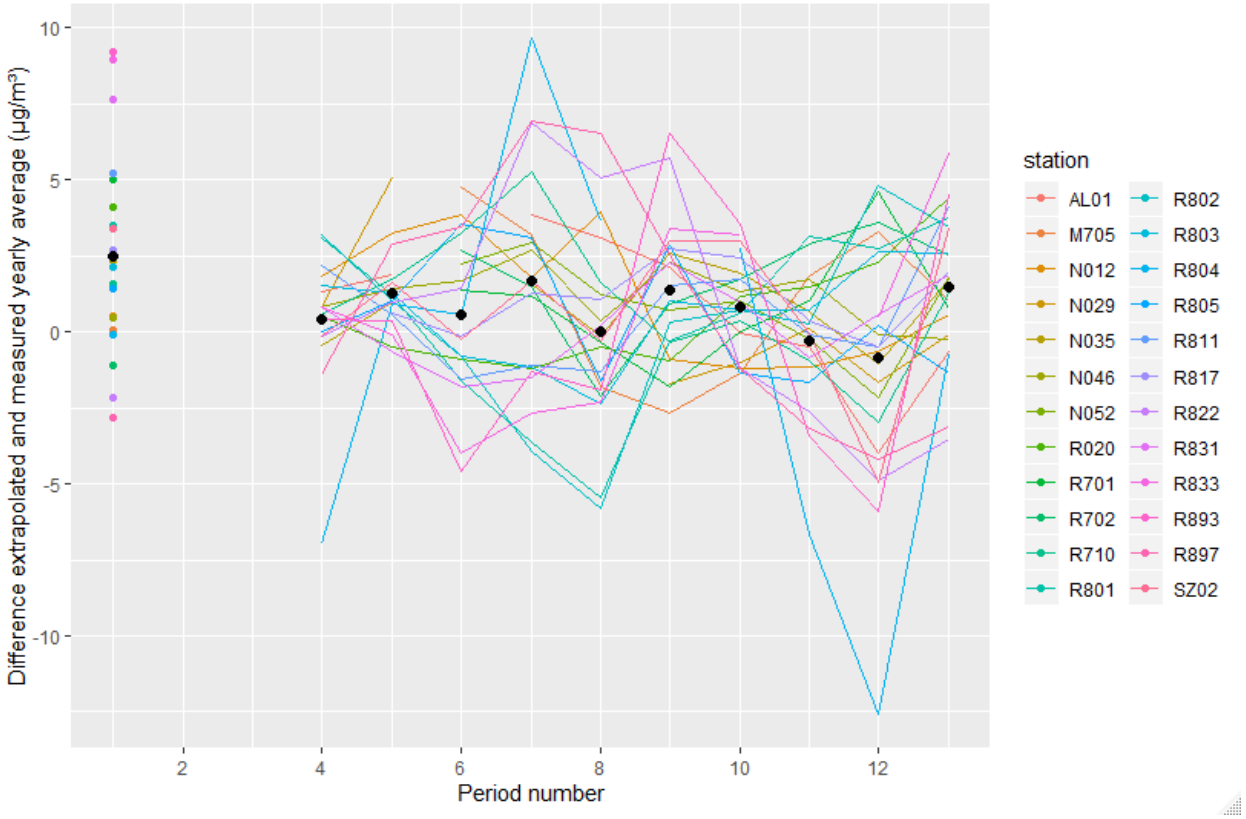

Figure S5. *Residuals for the sampler dataset (i.e. the difference between modelled and measured yearly averaged NO_2 values as calculated by Eq(10) in the main text). Residuals are displayed per 4-week period over the year 2018. Black dots denote the average values per period for all stations. Residuals from periods 2 and 3 are missing due to absence of sampler data .*

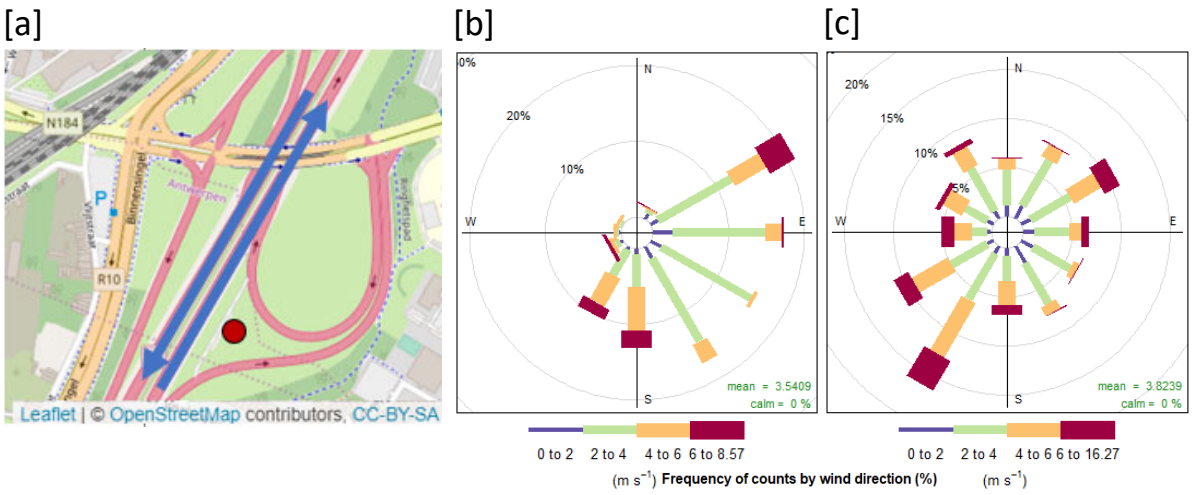

Figure S6. *The highway station R804 shows a high model error over period 12 in 2018. [a] Location of highway station R804 (red dot) and local traffic flows (blue arrows). [b] Wind rose only for period 12 in 2018 [c] Wind rose for the whole of 2018. Colors show fraction of winds at a certain wind speed for each direction.*